# Electronic supplementary information (ESI)

## ESI Table 1 Scoring of disease activity index

| Score | Weight loss (%) | Stool consistency | Occult blood or gross bleeding |
|---|---|---|---|
| 0 | None | Normal | Negative |
| 1 | 1-5 | | |
| 2 | 5-10 | Loose stool | Hemoccult positive |
| 3 | 10-15 | | |
| 4 | > 15 | Diarrhea | Gross bleeding |

Note: Disease activity index = (combined score of weight loss, stool consistency, and occult blood or gross bleeding)/3

## ESI Table 2 Grading of histopathology of colon tissues

| Score | Severity of inflammation | Depth of injury | Crypt damage |
|---|---|---|---|
| 0 | None | None | None |
| 1 | Slight | Mucosa | Basal 1/3 damaged |
| 2 | Moderate | Mucosa and submucosa | Basal 2/3 damaged |
| 3 | Severe | Transmural | Only surface epithelium intact |
| 4 | – | – | Entire crypt and epithelium lost |

Note: The histological score for each rat was a sum of the score of severity of inflammation, depth of injury, and crypt damage.

## ESI Table 3 Selected preclinical and clinical studies reporting a significant increase in gut *Akkermansia muciniphila* in relation with disease

| Study | Country | Disease model/disease | Characteristics of subjects and sample size | Sequencing method |
|---|---|---|---|---|
| **Rodent models** | | | | |
| Zhou et al. (2023)[1] | China | Dextran sulfate sodium (DSS)-induced ulcerative colitis (UC) | 6–8 weeks old female C57BL/6 mice; 6 UC and 6 control | 16S rRNA (V3-V4 region); Illumina HiSeq 2500; Paired-end 250 bp /300 bp |
| Lu et al. (2023)[2] | China | DSS-induced UC | 5 weeks old male C57BL/6 mice; 8 UC and 8 control | 16S rRNA (V3-V4 region); Illumina Miseq PE300 |
| Gao et al. (2023)[3] | China | DSS-induced UC | 8 weeks old female C57BL/6 mice; 6 UC and 6 control | 16S rRNA (V3-V4 region); Illumina MiSeq PE300 |
| Jiang et al. (2022)[4] | China | DSS-induced UC | 7 weeks old male C57BL/6J mice; 5 UC and 5 control | 16S rRNA (V3-V4 region); Illumina NovaSeq; Paired-end 250 bp |
| Huang et al. (2022)[5] | China | DSS-induced UC | 4–5 weeks old male C57BL/6N mice; 8 UC and 8 control | 16S rRNA (V3-V4 region); Illumina; Paired-end 2 × 250 bp |
| Huang et al. | China | DSS-induced UC | 8 weeks old male C57BL/6J mice; 15 UC and 15 control | 16S rRNA (V3-V4 region); |

| | | | | |
|---|---|---|---|---|
| (2022)[6] | | | | Illumina NovaSeq 6000 |
| Hu et al. (2022)[7] | China | DSS-induced UC | 6–8 weeks old male C57BL/6 mice; 6 UC and 6 control | 16S rRNA (V3-V4 region); Illumina Miseq PE300 |
| **Humans** | | | | |
| Jangi et al. (2016)[8] | USA | Multiple sclerosis | 60 patients and 43 healthy subjects | 16S rRNA (V4 region); Illumina MiSeq; Paired-end 2 × 150 bp |
| Cekanaviciute et al. (2017)[9] | USA | Multiple sclerosis | 71 patients and 71 healthy subjects | 16S rRNA |
| Zhang et al. (2020)[10] | China | Parkinson's disease | 63 patients and 137 healthy subjects | 16S rRNA (V4 region); Illumina HiSeq PE250 |
| Tan et al. (2021)[11] | Malaysia | Parkinson's disease | 104 patients and 96 healthy subjects | 16S rRNA (V3-V4 region); Illumina Hiseq 2500 |


1. Z. Zhou, W. He, H. Tian, P. Zhan and J. Liu, Thyme (Thymus vulgaris L.) polyphenols ameliorate DSS-induced ulcerative colitis of mice by mitigating intestinal barrier damage, regulating gut microbiota, and suppressing TLR4/NF-κB-NLRP3 inflammasome pathways, *Food Funct*, 2023, **14**, 1113-1132.
2. H. Lu, M. Shen, Y. Chen, Q. Yu, T. Chen and J. Xie, Alleviative effects of natural plant polysaccharides against DSS-induced ulcerative colitis via inhibiting inflammation and modulating gut microbiota, *Food Res Int*, 2023, **167**, 112630.
3. H. Gao, Y. Li, J. Xu, X. Zuo, T. Yue, H. Xu, J. Sun, M. Wang, T. Ye, Y. Yu and Y. Yao, Saccharomyces boulardii protects against murine experimental colitis by reshaping the gut microbiome and its metabolic profile, *Front Microbiol*, 2023, **14**, 1204122.
4. K. Jiang, D. Wang, L. Su, X. Liu, Q. Yue, B. Li, K. Li, S. Zhang and L. Zhao, Structural characteristics of locust bean gum hydrolysate and its alleviating effect on dextran sulfate sodium-induced colitis, *Front Microbiol*, 2022, **13**, 985725.
5. Y. Y. Huang, Y. P. Wu, X. Z. Jia, J. Lin, L. F. Xiao, D. M. Liu and M. H. Liang, Lactiplantibacillus plantarum DMDL 9010 alleviates dextran sodium sulfate (DSS)-induced colitis and behavioral disorders by facilitating microbiota-gut-brain axis balance, *Food Funct*, 2022, **13**, 411-424.
6. Y. Huang, Y. Zheng, F. Yang, Y. Feng, K. Xu, J. Wu, S. Qu, Z. Yu, F. Fan, L. Huang, M. Qin, Z. He, K. Nie and K. F. So, Lycium barbarum Glycopeptide prevents the development and progression of acute colitis by regulating the composition and diversity of the gut microbiota in mice, *Front Cell Infect Microbiol*, 2022, **12**, 921075.
7. Y. Hu, X. Jin, F. Gao, T. Lin, H. Zhu, X. Hou, Y. Yin, S. Kan and D. Chen, Selenium-enriched Bifidobacterium longum DD98 effectively ameliorates dextran sulfate sodium-induced ulcerative colitis in mice, *Front Microbiol*, 2022, **13**, 955112.
8. S. Jangi, R. Gandhi, L. M. Cox, N. Li, F. von Glehn, R. Yan, B. Patel, M. A. Mazzola, S. Liu, B. L. Glanz, S. Cook, S. Tankou, F. Stuart, K. Melo, P. Nejad, K. Smith, B. D. Topcuolu, J. Holden, P. Kivisakk, T. Chitnis, P. L. De Jager, F. J. Quintana, G. K. Gerber, L. Bry and H. L. Weiner, Alterations of the human gut microbiome in multiple sclerosis, *Nat Commun*, 2016, **7**, 12015.

9. E. Cekanaviciute, B. B. Yoo, T. F. Runia, J. W. Debelius, S. Singh, C. A. Nelson, R. Kanner, Y. Bencosme, Y. K. Lee, S. L. Hauser, E. Crabtree-Hartman, I. K. Sand, M. Gacias, Y. Zhu, P. Casaccia, B. A. C. Cree, R. Knight, S. K. Mazmanian and S. E. Baranzini, Gut bacteria from multiple sclerosis patients modulate human T cells and exacerbate symptoms in mouse models, *Proc Natl Acad Sci U S A*, 2017, **114**, 10713-10718.
10. F. Zhang, L. Yue, X. Fang, G. Wang, C. Li, X. Sun, X. Jia, J. Yang, J. Song, Y. Zhang, C. Guo, G. Ma, M. Sang, F. Chen and P. Wang, Altered gut microbiota in Parkinson's disease patients/healthy spouses and its association with clinical features, *Parkinsonism Relat Disord*, 2020, **81**, 84-88.
11. A. H. Tan, C. W. Chong, S. Y. Lim, I. K. S. Yap, C. S. J. Teh, M. F. Loke, S. L. Song, J. Y. Tan, B. H. Ang, Y. Q. Tan, M. T. Kho, J. Bowman, S. Mahadeva, H. S. Yong and A. E. Lang, Gut Microbial Ecosystem in Parkinson Disease: New Clinicobiological Insights from Multi-Omics, *Ann Neurol*, 2021, **89**, 546-559.

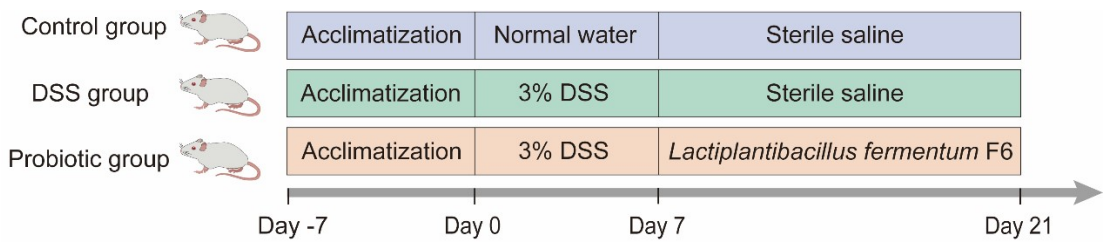


**ESI Fig. 1 Design of animal trial.** Twenty-four 8-week-old specific pathogen-free male Wistar wild-type rats were randomly divided into three groups: control, Dextran sulfate sodium (DSS), and probiotic groups (n = 8). All rats were acclimatized to the animal house environment for seven days before the trial. The rat colitis model was induced by administering DSS in their drinking water (DSS and probiotic groups) ad libitum for seven days. After that, rats in the control and DSS groups were daily gavaged with 2 mL sterile saline for 14 days, while rats in the probiotic group were daily gavaged with 2 mL sterile saline containing probiotic *Lactiplantibacillus fermentum* F6 ($4 \times 10^9$ CFU/day) for 14 days.

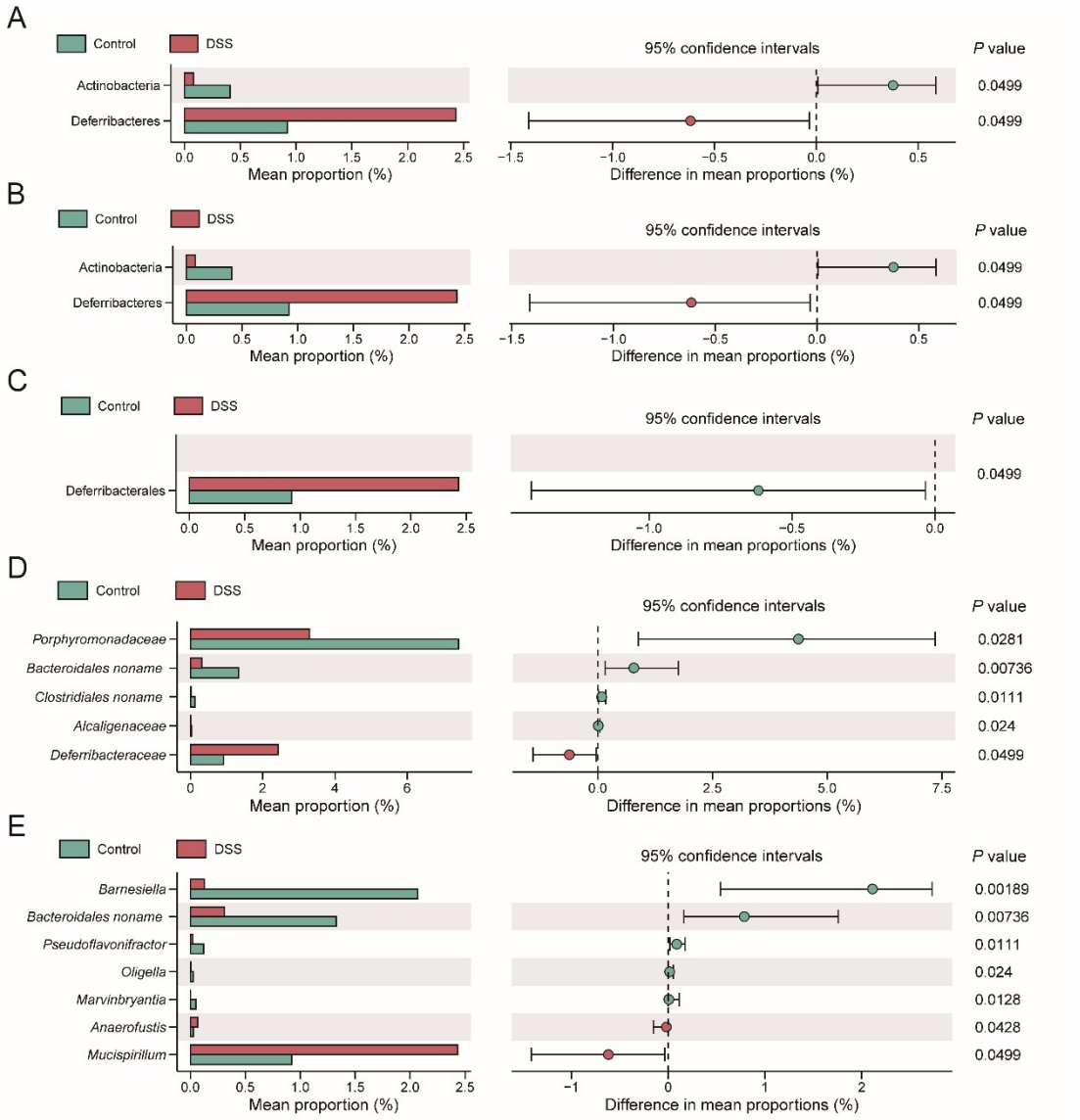


**ESI Fig. 2 Alterations of the gut microbial composition in rats with colitis.** Significant differentially abundant bacterial taxa between the control and Dextran sulfate sodium (DSS) groups at the (**A**) phylum, (**B**) class, (**C**) order, (**D**) family, and (**E**) genus levels; evaluated by Wilcoxon rank-sum test.

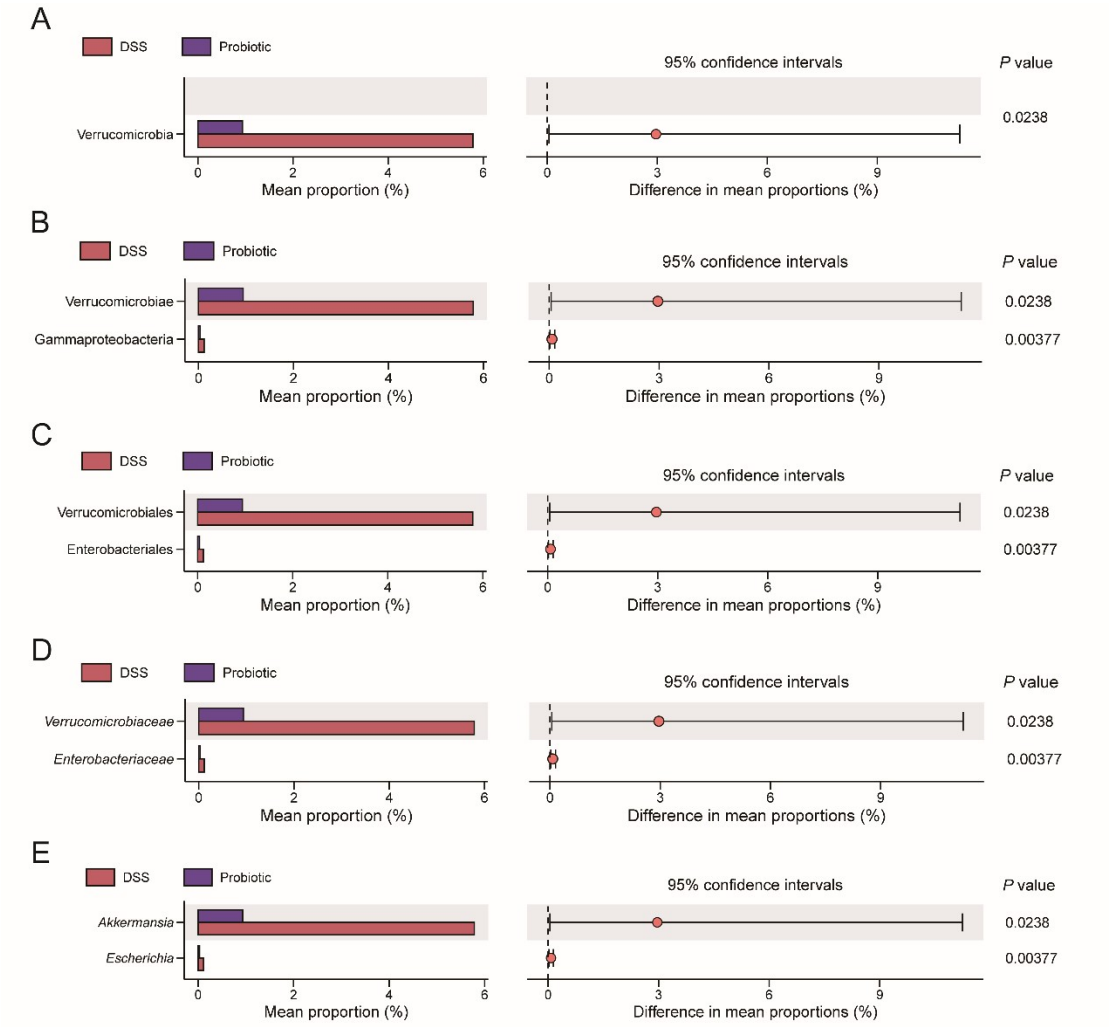


**ESI Fig. 3 Alterations of the gut microbial composition in colitis rats after the probiotic intervention.** Significant differentially abundant bacterial taxa between the Dextran sulfate sodium (DSS) and probiotic groups at the (**A**) phylum, (**B**) class, (**C**) order, (**D**) family, and (**E**) genus levels; evaluated by Wilcoxon rank-sum test.

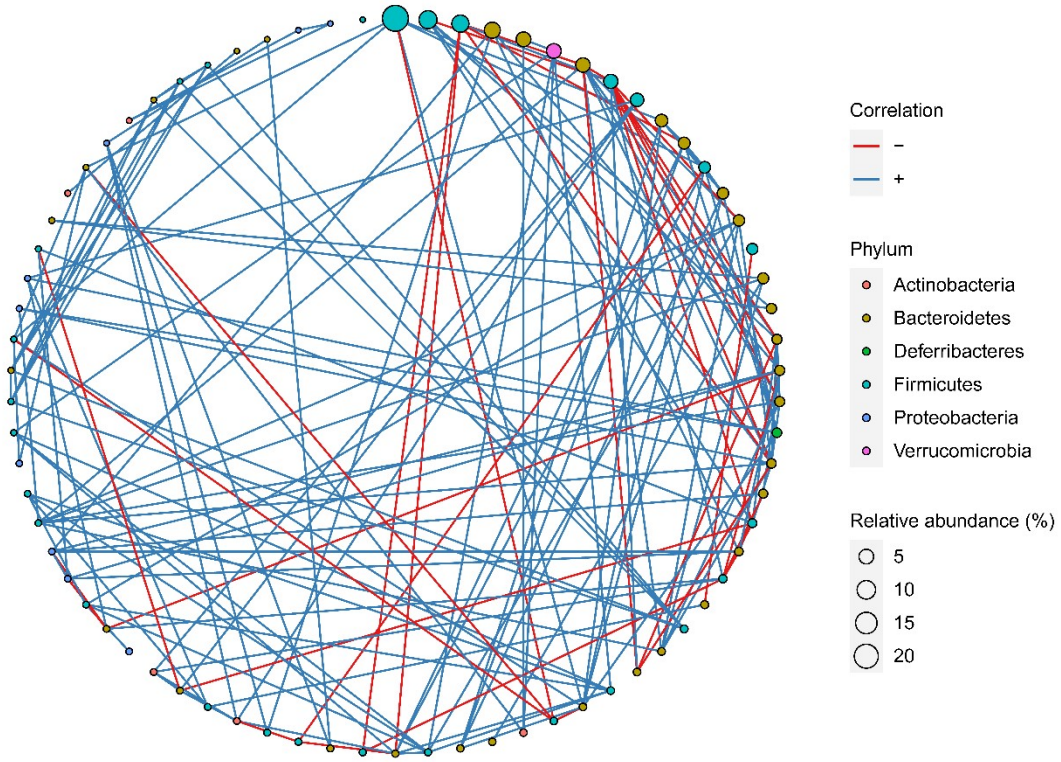


**ESI Fig. 4 Interconnectedness of the gut microbiota of the control group based on the Spearman correlation algorithms.** The node size represents the mean relative abundance of each bacterial taxon (arranged clockwise in descending order of abundance along the circle), and the node color indicates phylum. The red and blue lines between nodes represent negative and positive associations, respectively. Only correlations with absolute values of correlation coefficients above 0.6 and *P* values less than 0.05 were shown.

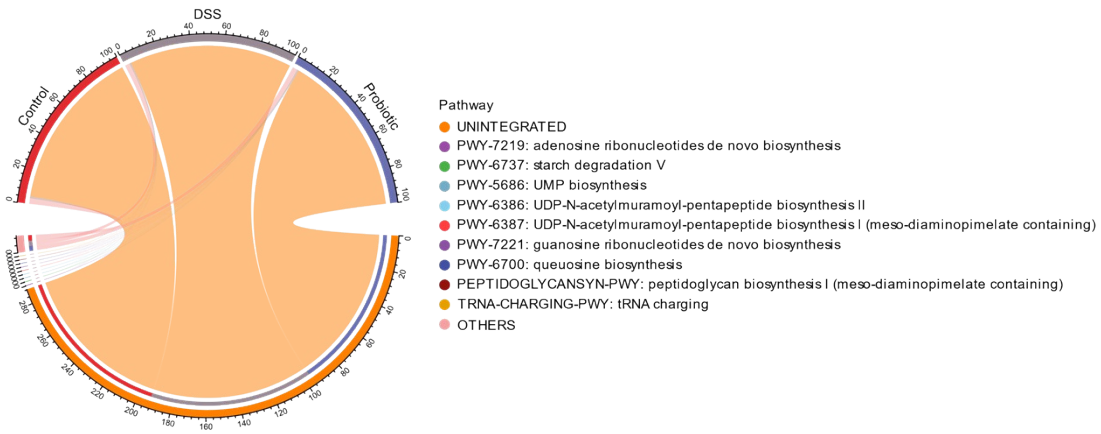


**ESI Fig. 5 Distribution of MetaCyc pathways encoded by the gut microbiota of the control, Dextran sulfate sodium (DSS), and probiotic groups.** The upper half circle represents the three treatment groups, while the lower half circle represents the overall composition of the MetaCyc pathways across all groups.

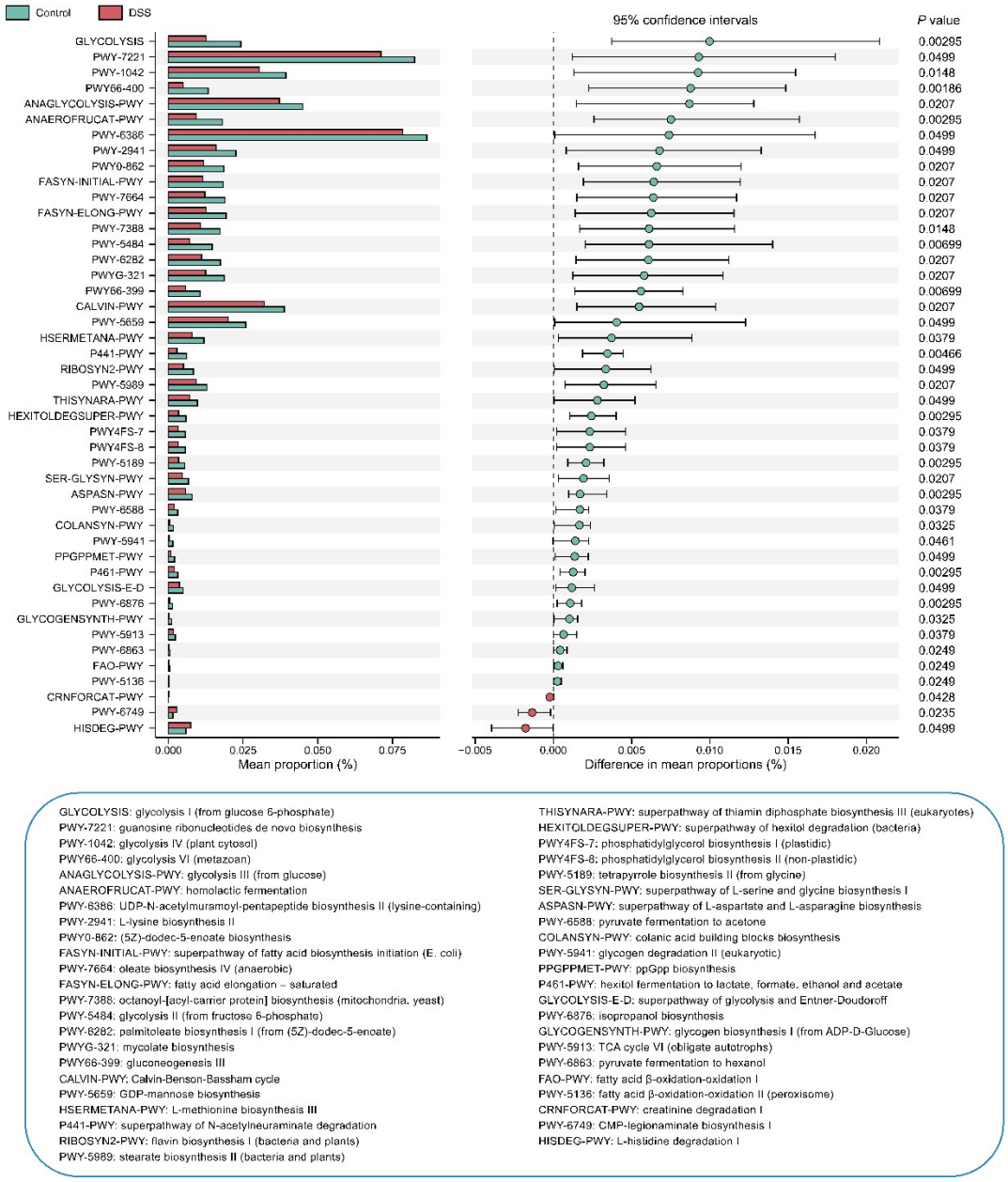


**ESI Fig. 6 Differences in gut microbiota-encoded MetaCyc pathways between the control and dextran sulfate sodium (DSS) groups.** Differentially abundant MetaCyc pathways between the control and DSS groups are shown. Significant differences were evaluated by Wilcoxon rank-sum test.

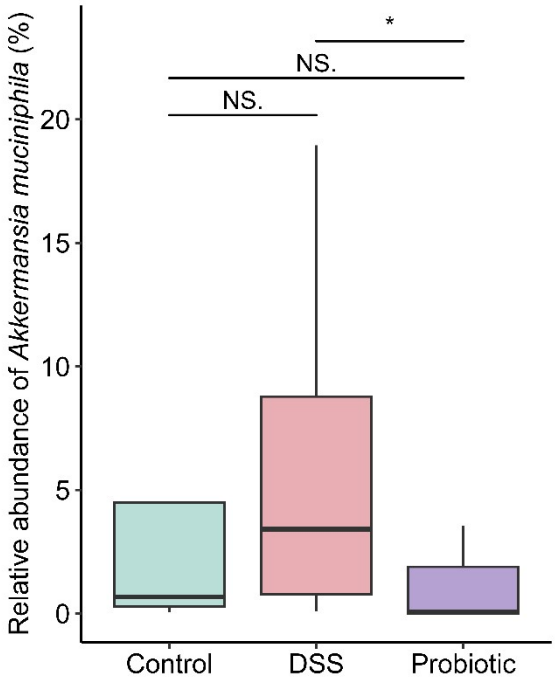


**ESI Fig. 7 Distribution of intestinal *Akkermansia muciniphila* in the fecal metagenome of the control, Dextran sulfate sodium (DSS), and probiotic groups.** Statistical differences in the relative abundance of *Akkermansia muciniphila* between groups were evaluated by Kruskal-Wallis test followed by Wilcoxon rank-sum test. *$P < 0.05$ and NS (not significant).